Inorg. Chem. **2005**, *44*, 9554–9560

Characterization and ab Initio XRPD Structure Determination of a Novel Silicate with *Vierer* Single Chains: The Crystal Structure of $NaYSi_2O_6$

Daniel M. Tobbens,*,† Volker Kahlenberg,† and Reinhard Kaindl§

Institute of Mineralogy and Petrography, University of Innsbruck, Innrain 52, A-6020 Innsbruck, Austria, and Christian-Doppler-Laboratory for Advanced Hard Coatings at the Institute of Mineralogy and Petrography, University of Innsbruck, Innrain 52, A-6020 Innsbruck, Austria

Received August 17, 2005

The crystal structure of a sodium yttrium silicate with composition $NaYSi_2O_6$ has been determined from laboratory X-ray powder diffraction data by simulated annealing, and has been subsequently refined with the Rietveld technique. The compound is monoclinic with space group $P2_1/c$ and unit cell parameters of $a = 5.40787(2)$ Å, $b = 13.69784(5)$ Å, $c = 7.58431(3)$ Å, and $\beta = 109.9140(3)°$ at 23.5 °C ($Z = 4$). The structure was found to be a single-chain silicate with a chain periodicity of four. The two symmetry dependent $[Si_4O_{12}]$ chains in the unit cell are parallel to ***c***. A prominent feature is the strong folding of the crankshaft-like chains within the ***b***,***c***-plane resulting in intrachain Si–Si–Si angles close to 90°. The coordination of the Y^{3+} ions by O^{2-} is 7-fold in the form of slightly irregular pentagonal bipyramids, with oxygen atoms from four different chains contributing to the coordination polyhedron. Na^+ ions are irregularly coordinated by 10 oxygens from two neighboring chains. No disorder of Na^+ and Y^{3+} between the two nontetrahedral cation sites could be observed. Furthermore, micro-Raman spectra have been obtained from the polycrystalline material.

Introduction

Sodium yttrium silicates are of considerable importance in materials science. For example, reports on the high ionic conductivity in $Na_5YSi_4O_{12}$ and $Na_3YSi_6O_{15}$ have stimulated interest in the synthesis and fabrication of these phases,[1−5] in which the Na ions can migrate via channels present in the silicate framework. Furthermore, the search for new inorganic phosphors resulted in investigations on the photoluminescence characteristics in $Na_3YSi_3O_9$ after doping with Eu^{3+} ions.[6]

Apart from their relevance in technology, sodium yttrium silicates are also interesting from a structural point of view. The incorporation of Y^{3+} into the silicate structures results in several unusual structure types. $Na_3YSi_3O_9$, for example, contains spiral 24*er* single chains.[7] To the best of our knowledge, these tetrahedral chains exhibit the highest value for chain periodicity in silicates observed so far. On the other hand, $Na_3YSi_6O_{15}$ occurs in two different modifications, including a form in which rather uncommon $[Si_6O_{15}]^{6-}$ double *dreier* rings can be found.[5]

A comprehensive study on the phase relationships in the system $Na_2O-Y_2O_3-SiO_2$ has been performed by Cervantes-Lee.[8] According to his results, six different ternary crystalline phases have to be distinguished. In addition to the compounds mentioned above, the existence of the following phases was proved: $NaY_9Si_6O_{26}$, $Na_3YSi_2O_7$, $Na_9YSi_6O_{18}$, and $NaYSi_2O_6$. The crystal structures of the first two compounds have been already determined. Whereas $NaY_9Si_6O_{26}$ belongs to the apatite structure family,[9] $Na_3YSi_2O_7$ represents a soro-silicate

* To whom correspondance should be addressed. E-mail: daniel.toebbens@uibk.ac.at. Phone: +43 (0)512 507 5532. Fax: +43 (0)512 507 2926.
† Institute of Mineralogy and Petrography, University of Innsbruck.
§ Christian-Doppler-Laboratory for Advanced Hard Coatings at the Institute of Mineralogy and Petrography, University of Innsbruck.

(1) Shannon, R. D.; Taylor, B. E.; Gier, T. E.; Chen, H. Y.; Berzins, T. *Inorg. Chem.* **1978**, *17*, 958−964.
(2) Hong, H.; Kafalas, J. A.; Bayard, M. *Mater. Res. Bull.* **1978**, *13*, 757−761.
(3) Beyeler, H. U.; Shannon, R. D.; Chen, H. Y. *Solid State Ionics* **1981**, *3*−*4*, 223−226.
(4) Yamashita, K. *J. Mater. Res.* **1998**, *13*, 3361−3364.
(5) Haile, S. M.; Maier, J.; Wuensch, B. J. *Acta Crystallogr.* **1995**, *B51*, 673−680.
(6) Kim, C. H.; Park, H. L.; Mho, S. *Solid State Commun.* **1996**, *101*, 109−113.
(7) Maksimov, B. A.; Kalinin, V. P.; Merinov, B. V.; Ilyukhin, V. V.; Belov, N. V. *Dokl. Akad. Nauk SSSR* **1980**, *252*, 875−879.
(8) Cervantes Lee, F. J. Studies in oxide chemistry. Ph.D. Thesis, University of Aberdeen, Aberdeen, Scotland, 1981.

10.1021/ic051401o CCC: $30.25
Published on Web 11/05/2005

Table 1. Experimental Conditions and Rietveld Analysis

radiation type, source	X-ray, Cu $K\alpha_1$
generator settings	40 kV, 40 mA
discriminator	primary beam, curved Ge(111) monochromator
detector	linear PSD, 6° width
effective μt	2.2
data collection temperature	23.5(5) °C
range in 2θ	2.0−131°
PSD step size	0.1°, 80 s/step
internal integration step size	0.01°
space group	$P12_1/c1$
chemical composition	$NaYSi_2O_6$, Z = 4
no. of contributing reflections	952 total, 364 effective
no. of structural parameters	40
no. of profile parameters	29
R_{wp}	7.13%
R_{exp}	4.34%
R_{Bragg}	2.81%

with discrete $[Si_2O_7]$ units.[10] On the other hand, the structures of the latter two silicates remain to be solved.

The present study is aimed at characterizing the crystal structure of $NaYSi_2O_6$ in detail. Because of the fact that $NaYSi_2O_6$ is known to melt incongruently at about 1450 °C,[8] no single crystals could be obtained, and thus the structure determination was performed using powder diffraction data obtained from a polycrystalline specimen. The characterization is complemented by Raman spectroscopical studies.

Experimental Section

Starting materials for the synthesis of $NaYSi_2O_6$ were Na_2CO_3 (Merck, p.a.), Y_2O_3 (Johnson Matthey, 99.99%), and fine-grained quartz powder (Merck, p.a.). One gram of the reagents was carefully mixed in an agate mortar under acetone, and pressed into disks. The pellets confined in open 50 mL platinum crucibles were heated in air from 250 to 1150 °C at 5 °C/min in a resistance heated furnace, and subsequently held at this temperature for 4 days. Finally, the reaction was quenched. The product was characterized by X-ray powder diffraction. The firing procedure at 1150 °C was repeated until no differences between the powder patterns of subsequent cycles could be detected. For chemical analyses, a standardless energy dispersive electron probe microanalysis was performed using a JEOL JXA-8100 superprobe with a lateral resolution of 1 μm^3 (10 kV, 20 nA). The density of the material was determined to be 3.4(1) g/cm^3 using a glass bottle pycnometer and water as a working fluid.

X-ray powder diffraction data for structure determination and refinement have been collected on a Stoe STADI-MP diffractometer in flat-plate transmission geometry using a sample of 6 mm diameter prepared between two thin foils. The diffractometer is equipped with an asymmetric primary beam Ge(111) monochromator (yielding a strictly monochromatic Cu $K\alpha_1$-radiation) and a linear PSD with a 6° detector range. The effective value of 2.2 for the product μt (μ = linear absorption coefficient; t = sample thickness) used for the absorption correction was determined experimentally from the intensity ratios at $\theta = 0°$ with and without the sample. Details of the data collection and the refinement are given in Table 1.

Confocal Raman spectra of polycrystalline $NaYSi_2O_6$ were obtained with a Horiba Jobin Yvon LabRam-HR 800 Raman microspectrometer. Spectra were excited at room temperature with the 488 nm line of a 30 mW Ar^+ laser through an Olympus 100× objective. The laser spot on the surface had a diameter of approximately 1 μm and a power of 5 mW. Light was dispersed by a holographic grating with 1800 grooves/mm. A spectral resolution of about 1.8 cm^{-1} was experimentally determined by measuring the Rayleigh line. The dispersed light was collected by a 1024 × 256 open-electrode CCD detector. The confocal pinhole was set to 1000 μm. The depth resolution of this true-confocal configuration is usually better than 2 μm. Spectra were recorded unpolarized. The scanning mode was selected in order to avoid steplike mismatches between neighboring spectral windows, probably occurring in samples with intense and uneven background, and to maximize the signal-to-noise ratio.[11,12] All spectra were baseline-corrected by subtracting line segments, and were fitted to Gauss−Lorentz functions. Deviations between the measured full width at half-maximum (fwhm) and the so-called apparatus function mathematical corrected fwhm[13−15] were less than 0.5 cm^{-1} and hence not corrected. Wavenumber calibration was done by regular measuring of the Rayleigh line. The accuracy achieved by this method was better than 0.5 cm^{-1}.

Structure Solution and Refinement

A comparison with the reported X-ray powder diffraction pattern of $NaYSi_2O_6$ (PDF-4 entry 35-0407) revealed the presence of several additional low-intensity lines. There are at least two possible explanations for this result: (a) the powder pattern of $NaYSi_2O_6$ is more complex, i.e., weak reflections have been overlooked in the previous study, and/or (b) the specimen contains impurities. To settle this question, we studied the sample using an electron microprobe offering a space-resolved determination of the chemical composition analysis. This energy dispersive analysis revealed the presence of at least two phases. The main silicate phase exhibited a Na:Y ratio close to 1:1. Grains of a minor phase were sodium-free, indicating the existence of a pure Y-silicate.

Peak positions for unit cell determination were determined by profile fitting using WinXPow.[16] Indexing of the reflections was done with the Crysfire suite[17] in combination with Chekcell.[18] The symmetry was found to be monoclinic with extinctions indicating a primitive unit cell and a 2_1-screw axis. A number of weak unindexed reflections were attributed to the second minor phase mentioned above. In good agreement with the chemical analysis, this compound could be identified as the Y-analogue of Keivyite ($Er_2Si_2O_7$, ICSD entry 74779). According to the final Rietveld analysis, this compound's total amount corresponds to about 1.3(1) wt %. A remaining single unexplained peak at 45.68(2)° indicates the presence of a very small amount of a 3rd phase that could not be identified.

A LeBail refinement performed with the program FullProf[19] provided starting values for the unit cell metric as well as

(9) Gunawardane, R. P.; Howie, R. A.; Glasser, F. P. *Acta Crystallogr.* **1982**, *B38*, 1564−1566.
(10) Merinov, B. V.; Maksimov, B. A.; Nelov, N. V. *Dokl. Akad. Nauk SSSR* **1981**, *260*, 1128−1130.
(11) Knoll, P.; Singer, R.; Kiefer, W. *Appl. Spectrosc.* **1990**, *44* (4), 776−782.
(12) Nasdala, L.; Massonne, H.-J. *Eur. J. Mineral.* **2000**, *12* (2), 495−498.
(13) Irmer, G. *Exp. Tech. Phys.* **1985**, *33*, 301−306.
(14) Verma, P.; Abbi, S. C.; Jain, K. P. *Phys. Rev. B* **1995**, *51* (23), 16660−16667.
(15) Nasdala, L.; Wenzel, M.; Vavra, G.; Irmer, G.; Wenzel, T.; Kober, B. *Contrib. Mineral. Petrol.* **2001**, *141*, 125−144.
(16) *STOE WinXPow 2.10*; STOE & Cie GmbH: Darmstadt, Germany, 2004.
(17) Shirley, R. *The Crysfire 2002 System for Automatic Powder Indexing*, 2002.
(18) Laugier, J.; Bochu, B. *LMGP Suite of Programs for the Interpretation of X-ray Experiments*; ENSP/Laboratoire des Mate'riaux et du Ge'nie Physique: Saint Martin d'He'res, France; http://www.inpg.fr/LMGP.

background and peak width/shape parameters. These values were directly used for the subsequent structure solution. From the unit cell volume of 528.231(9) Å^3 with $Z = 4$, a density of 3.32 g/cm^3 results. This is in good agreement with the experimentally determined density of 3.4(1) g/cm^3.

Structure determination was performed by parallel simulated annealing using the program FOX.[20] For the starting model, the appropriate number of Na, Y, and Si atoms was placed in the unit cell. For each individual silicon atom, a tetrahedral coordination by four oxygen atoms was assumed (resulting in an oxygen excess compared to the assumed chemical composition). The program's dynamic occupancy correction was activated to allow for linkage between the SiO_4 tetrahedra. Anti-bump restraints were applied to all atoms with distances corresponding to the combined ionic radii. Annealing runs of 1 million trials each were done in those space groups compatible with the observed systematic extinction rules: $P2_1$ and $P2_1/m$. In each space group, various basic models of connections between SiO_4 tetrahedra were tested: insular SiO_4 tetrahedra, Si_2O_7 units, Si_4O_{13} groups, or Si_4O_{12} rings (the latter two for $P2_1$ only). Soft interatomic distance and angle constraints of 1.64 Å and 109.5°, respectively, were applied to the SiO_4 tetrahedra. No restrictions were utilized for the Si−O−Si angles. A reasonable structure solution concerning residuals and crystal chemistry was found in space group $P2_1$ from the approach using Si_2O_7 dimers. In this model, the Si_2O_7 units did connect to *vierer* single chains, resulting in the expected overall chemical composition. Of the four independent cation sites (in $P2_1$), the position of one Na atom had to be adjusted manually. Subsequent simulated annealing resulted in a further significant increase of the quality of the fit.

An inspection of the atomic coordinates of the model obtained from the structure determination using the MISSYM algorithm implemented in the program PLATON[21] revealed the existence of an additional *c*-glide plane. Therefore, the real space group symmetry of the structure is $P2_1/c$. Because of peak overlaps with reflections of the impurities, the systematic absences ($h0l$): $l = 2n + 1$ corresponding to this additional symmetry element could not be detected.

Final Rietveld refinement of the structure was done with FullProf using ionic structure factors and individual isotropic Debye−Waller factors. No constraints on interatomic distances or angles were applied during the structure refinement. Thompson−Cox−Hastings−Pseudo−Voigt functions were employed to describe the peak shape, including an asymmetry correction following Finger et al.[22] The background was modeled by linear interpolation between points with no or small peak intensity contribution. The experimentally determined absorption correction was applied to the data using the built-in function of the program for the Stoe transmission geometry. The minor phase $Y_2Si_2O_7$ was modeled by taking atomic positions from ICSD entry 74779, replacing Er^{3+} with Y^{3+}, coupling peak shape and width to the main phase, and refining scale factor and lattice parameters only. The structure refinement converged to residuals of $R_{wp} = 7.1\%$, $\chi^2 = 2.7$, and $R_{Bragg} = 2.8\%$ with an effective reflection/intensity-dependent parameter ratio of 9. The correction factor for estimated standard deviations of the refined parameters as proposed by Bérar[23] is 3.0. A graphical comparison between the observed and calculated powder patterns is given in Figure 1.

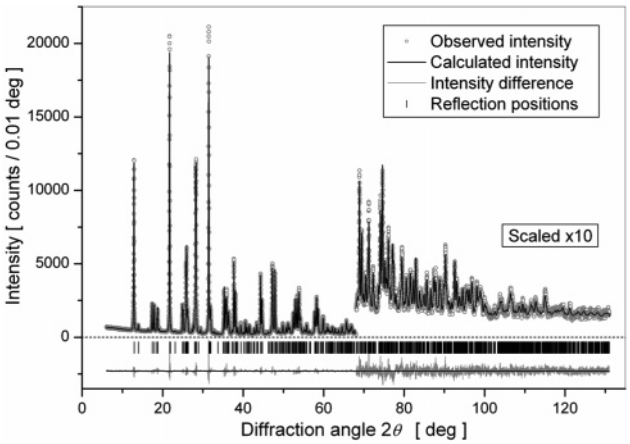

Figure 1. Observed (circles) and calculated (solid line) step intensities and their difference (line at bottom of figure) of $NaYSi_2O_6$. To obtain a more concise representation of the high-angle region, we have magnified the intensity in this area by a factor of 10. Peak positions permitted by unit-cell metric are indicated by tick marks (middle portion). Residuals of the Rietveld refinement are $R_{wp} = 7.1\%$, $\chi^2 = 2.7$.

Description of the Structure

The structure was found to be a *vierer* single chain silicate. According to the classification of Liebau,[24] the silicate chain can be described by the following structural formula: $\{\boldsymbol{uB},1^1_\infty\}$ $[^4Si_4O_{12}]$, denoting an unbranched (*uB*) single chain (1^1_∞) with a four-[SiO_4]-tetrahedra repetition unit, $[^4Si_4O_{12}]$. The two [Si_4O_{12}] chains in the unit cell are extending parallel to ***c***. The tetrahedra about the two symmetrically independent Si atoms comprising the chains are distorted: Si−O distances as well as the O−Si−O angles show a considerable scatter (Tables 3 and 4). However, in good agreement with the general crystal chemistry of silicates, the two nonbridging Si−O distances of the tetrahedra are considerably shorter than the two bonds between Si and the two bridging oxygen ligands ($\langle Si-O_{term}\rangle = 1.555(4)$ Å, $\langle Si-O_{brid}\rangle = 1.627(4)$ Å). The shortening of the nonbridging compared with the bridging bond lengths results from the stronger attraction between O and Si than between O and the Na/Y cations in the structure. The distortion can be expressed numerically using the mean quadratic elongation l as well as the angle variance σ^2.[25] These parameters have values of 1.015 and 1.011 as well as 61.20 and 50.64 for the two $Si1O_4$ and $Si2O_4$ polyhedra, respectively.

A prominent feature is the strong folding of the chains within the ***b***,***c***-plane with Si−Si−Si angles close to 90°, resulting in a crankshaft-type arrangement of the tetrahedra. Therefore, the intra-tetrahedral O−Si−O-angles within the chain are reduced (with an average value of 104.2(6)°). On the other hand, the O−Si−O angles involving only the nonbridging O atoms are significantly increased ($\langle O-Si-O\rangle = 122.2(9)°$). The pronounced undulation of the chains is also reflected in a low stretching factor[24] of $f_s = 0.70$.

(19) Rodríguez-Carvajal, J. *FullProf.2k*, version 3.20; LLB JRC: Gif-sur-Yvette Cedex, France, 2005.
(20) Favre-Nicolin, V.; Černý, R. *Z. Kristallogr.* **2004**, *219*, 847−856.
(21) Spek, A. L. *J. Appl. Crystallogr.* **2003**, *36*, 7−13.
(22) Finger, L. W.; Cox, D. E.; Jephcoat, A. P. *J. Appl. Crystallogr.* **1994**, *27*, 892−900.
(23) Bérar, J.-F.; Lelann, P. *J. Appl. Crystallogr.* **1991**, *24*, 1−5.
(24) Liebau, F. *Structural Chemistry of Silicates*; Springer-Verlag: Berlin, 1985.
(25) Robinson, K.; Gibbs, G. V.; Ribbe, P. H. *Science* **1971**, *171*, 560.

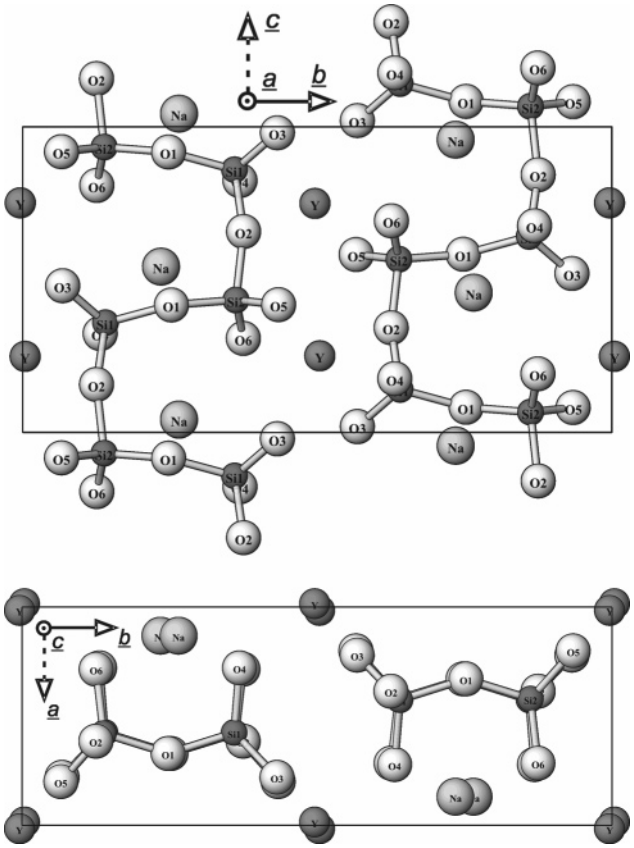

Figure 2. Crystal structure of $NaYSi_2O_6$ in projections along *a* and *c*, respectively. Note the large bond angle of 161.0(5)° at O2.

Linkage between the silicate anions is provided by the Y^{3+} and Na^+ cations occupying the voids between the chains. Projections of the whole crystal structure of $NaYSi_2O_6$ (prepared using the program ATOMS[26]) are given in Figure 2.

The coordination of the Y^{3+} ions by O^{2-} is 7-fold in the form of slightly irregular pentagonal bipyramids, with oxygen atoms from four different chains contributing to the coordination polyhedron. Na^+ ions are irregularly coordinated by 10 oxygens from two neighboring chains (Figure 3). No disorder of the cations among the two crystallographically different sites within the structure could be observed.

The structure is clearly dominated by the coordination requirements of the Y^{3+} cation. Bond valence analysis using the parameters implemented in FullProf[27,28] shows a valence sum of 2.94(2) valence units (v.u.) for the yttrium ion, closely matching the expected value of 3 v.u. To achieve this well-balanced situation, the O2 anion is shifted toward the Y^{3+} cation, transforming the octahedral coordination into a pentagonal bipyramid (Figure 3). This results in an increased bond angle at the corresponding oxygen ($\angle$Si1−O2−Si2 = 161.0(5)°) and a compression of those intra-tetrahedral angles that are part of the coordination sphere of Y^{3+} ($\angle$O2−Si1−O3 = 100.4(5)°, $\angle$O2−Si2−O5 = 100.4(6)°).

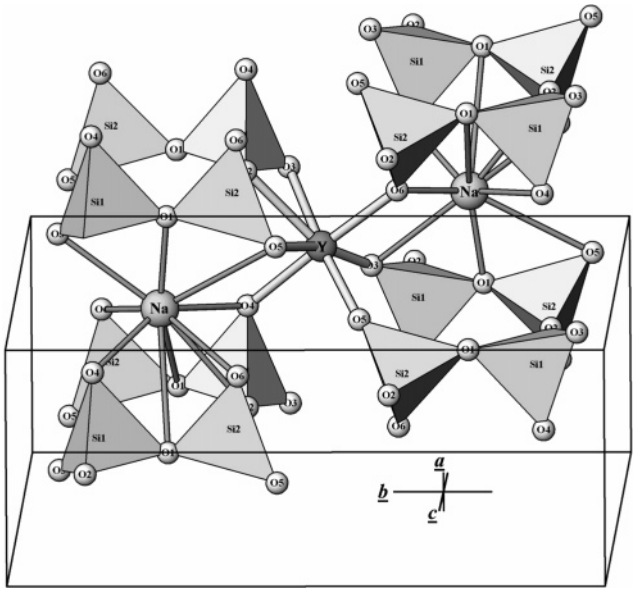

Figure 3. Coordination sphere of the Y^{3+} and Na^+ cations by the oxygen ligands.

Table 2. Structural Parameters of $NaYSi_2O_6$ in Space Group $P2_1/c$

atom[a]	*x*	*y*	*z*	B_{iso} (Å^2)
Y	0.9849(2)	0.0041(1)	0.2490(2)	0.58(2)
Na	0.1313(6)	0.2653(3)	0.0425(4)	1.97(8)
Si1	0.5752(6)	0.1404(2)	0.3589(4)	0.35(7)
Si2	0.5795(6)	0.3618(3)	0.4334(4)	0.50(7)
O1	0.6710(7)	0.2524(6)	0.4172(6)	2.55(12)
O2	0.6146(10)	0.1252(3)	0.1573(9)	3.42(16)
O3	0.7799(9)	0.0679(3)	0.4801(7)	0.73(15)
O4	0.2786(11)	0.1314(5)	0.3238(7)	1.21(16)
O5	0.7995(10)	0.4341(4)	0.4182(8)	3.00(19)
O6	0.2849(11)	0.3743(4)	0.3078(7)	1.82(17)
	a = 5.40787(2) Å		c = 7.58431(3) Å	
	b = 13.69784(5) Å		β = 109.9140(3)°	

[a] All atoms are located in fully occupied general positions (4*e*). The esds given in all tables should be multiplied by 3.0. See ref 23.

On the other hand, the coordination of the Na^+ cations is less well defined. To an upper limit of 3.4 Å, 10 oxygen ligands can be found (see Table 3). Because typical Na−O bond lengths average about 2.44 Å,[29] the longer bonds (between 3.1 Å and 3.4 Å) can be considered extremely weak. In more detail, the Na^+ ions reside above a square formed by four oxygens (2 × O4, 2 × O6) belonging to neighboring SiO_4 tetrahedra of only one chain. From the opposite side, an additional O1 atom of the second chain is involved in the coordination environment. If one focuses on this inner 5-fold coordination containing all short Na−O contacts, the coordination polyhedron could be described as a distorted tetragonal pyramid. The remaining longer Na−O distances are distributed over a wide range of values without any clear gaps. Therefore, five more oxygen atoms could be regarded as contributing to the coordination sphere: Two edges of the SiO_4 tetrahedra connected by the O1 anion extend the tip of the pyramid into an O5−O1−O3 edge. Furthermore, the corners connecting the four tetrahedra forming the base of the pyramid also contribute to the

(26) Dowty, E. *ATOMS for Windows*, version 3.2; Shape Software: Kingsport, TN, 1997.
(27) Brown, I. D.; Altermatt, D. *Acta Crystallogr.* **1985**, *B41*, 244−247.
(28) Brese, N. E.; O'Keeffe, M. *Acta Crystallogr.* **1991**, *B47*, 192−197.
(29) Wilson, A. J. C., Ed. *International Tables for Crystallography, Volume C: Mathematical, Physical and Chemical Tables*; Kluwer: Dordrecht, The Netherlands, 1995.

Table 3. Selected Interatomic Distances (Å)

bond	distance	bond	distance	bond	distance
Si1−O3	1.537(5)	Y−O5	2.212(7)	Na−O1	2.356(5)
Si1−O4	1.539(7)	Y−O3	2.243(5)	Na−O6	2.414(6)
Si1−O2	1.627(8)	Y−O6	2.247(6)	Na−O4	2.508(8)
Si1−O1	1.631(8)	Y−O4	2.296(6)	Na−O4	2.719(7)
		Y−O2	2.509(5)	Na−O3	2.906(6)
Si2−O6	1.562(6)	Y−O5	2.511(6)	Na−O6	2.919(7)
Si2−O5	1.582(7)	Y−O3	2.528(6)	Na−O2	3.118(6)
Si2−O1	1.596(9)			Na−O5	3.227(7)
Si2−O2	1.653(8)			Na−O1	3.313(4)
				Na−O1	3.371(6)

Table 4. Selected Bond Angles (deg)

bond	angle	bond	angle
O1−Si1−O2	104.1(6)	O1−Si2−O2	104.5(6)
O1−Si1−O3	110.4(6)	O1−Si2−O5	108.8(7)
O1−Si1−O4	109.8(6)	O1−Si2−O6	109.5(6)
O2−Si1−O3	100.4(5)	O2−Si2−O5	100.4(6)
O2−Si1−O4	106.8(7)	O2−Si2−O6	110.6(5)
O3−Si1−O4	123.2(6)	O5−Si2−O6	121.5(6)
Si1−O1−Si2	145.7(5)	Si1−O2−Si2	161.0(5)

Table 5. Raman Bands (cm^{-1}) and Relative Intensities[a] of Polycrystalline $NaYSi_2O_6$

Raman shift	intensity	Raman shift	intensity
106	5	484	14
116	7	548	1
136	4	561	18
158	2	622	42
174	13	750	7
202	18	905	5
264	7	930	7
303	46	971	3
341	16	1004	100
360	13	1022	110
384	10	1039	37
407	11	1064	6
431	3	1107	5
449	10		

[a] Integrated relative intensities in percent have been normalized to the band with the highest peak intensity at 1004 cm^{-1}.

coordination. The complete coordination polyhedron (including all 10 oxygen atoms) can be characterized as a distorted disphenoide with two truncated corners. Bond valence sum calculations show that Na is considerably underbonded (BVS = 0.83(1) v.u.), indicating that the sodium cations are exposed to a tensional strain and do not fit so well into the cavities between the tetrahedral chains. This observation is also reflected in the large Debye−Waller factor observed for the Na atoms.

It should be noted that those oxygen atoms with the highest Debye−Waller factors all belong to the $Si2O_4$ tetrahedron. Moreover, the Debye−Waller factor of Si2 is higher than the corresponding value for Si1. This may point to a certain degree of displacement disorder of this tetrahedron. A more detailed analysis, however, was not possible from the powder diffraction data.

Raman Spectroscopy

The Raman spectrum of $NaYSi_2O_6$ is displayed in Figure 4. Numerous bands in the low-, mid-, and high-wavenumber range were recorded. Position and relative intensities normalized to the band with the highest peak intensity at 1004 cm^{-1}

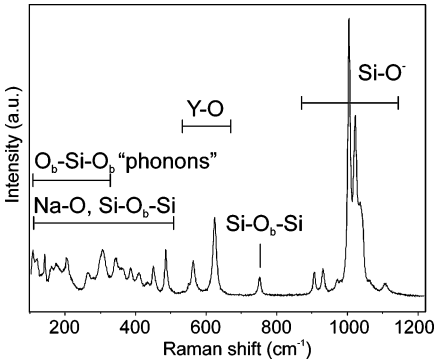

Figure 4. Raman spectra of $NaYSi_2O_6$. Band assignment is discussed in text. Raman shifts and relative intensities of individual bands are given in Table 5.

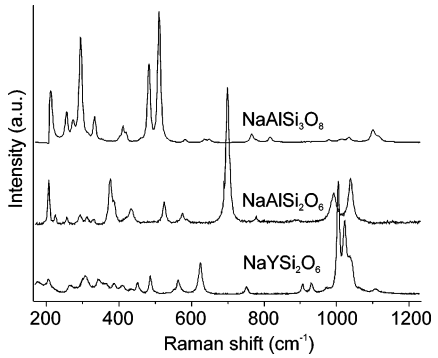

Figure 5. Comparison of the Raman spectra of $NaYSi_2O_6$, $NaAlSi_2O_6$ (jadeite), and $NaAlSi_3O_8$ (albite).

are given in Table 5. Symmetric Si−O^- stretching vibrations of SiO_4 groups with nonbridging oxygens emerge in alkali silicates with different contents of metal oxides in the high-wavenumber range 850−1250 cm^{-1}.[30,31] Bands in the intermediate-wavenumber range 400−800 cm^{-1} result from symmetric bending vibrations of the Si−O−Si bridging oxygens between adjacent SiO_4 tetrahedra. Below 400 cm^{-1}, bands are mainly caused by lattice vibrations of the framework and cation−oxygen bonding. In yttrium orthosilicate crystals, vibration bands in the 500−700 cm^{-1} range are generally characteristic for the YO_6 octahedra, but have also been observed for 6+1 coordination similar to the one discussed here.[32] Compared to jadeite, a chemically related pyroxene-type sodium aluminum silicate ($NaAlSi_2O_6$),[33] the band indicative of the strong Si−O−Si bridging vibration around 700 cm^{-1} is weaker and shifted to higher wavenumbers (see Figure 5). The comparable large number of medium to weak bands below 400 cm^{-1} in jadeite and $NaYSi_2O_6$ can probably be attributed to the existence of chain-type anions in both compounds. Raman bands of $NaYSi_2O_6$ in this region, which are characteristic for long-distance order lattice vibrations (phonons), are lower in intensity compared to the tectosilicate albite ($NaAlSi_3O_8$), consistent with the lower SiO_4 connectivity in jadeite and $NaYSi_2O_6$[34,35] (see Figure

(30) You, J.-L.; Jiang, G.-C.; Hou, H.-Y.; Chen, H.; Wu, Y.-Q.; Xu, K.-D. *J. Raman Spectrosc.* **2005**, *36*, 237−249.
(31) Akaogi, M.; Ross, N. L.; McMillan, P.; Navrotsky, A. *Am. Mineral.* **1984**, *69* (5−6), 499−512.
(32) Campos, S.; Denoyer, A.; Jandl, S.; Viana, B.; Vivien, D.; Loiseau, P.; Ferrand, B. *J. Phys. Condens. Mater.* **2004**, *16*, 4579−4590.
(33) Smith, D. C.; Gendron, F. *J. Raman Spectrosc.* **1997**, *28*, 731−738.

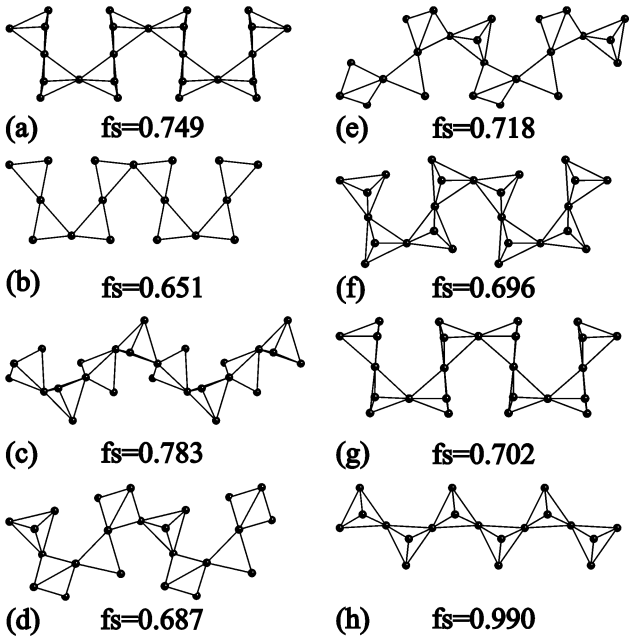

Figure 6. Comparison between *vierer* single chains and their stretching factors f_s in different silicate structures: (a) batisite, (b) haradaite, (c) krauskopfite, (d) leucophanite, (e) taikanite, (f) $Na_2Cu_3[Si_4O_{10}]$, and (g) $NaYSi_2O_6$. The almost completely stretched *zweier* single chain observed in pyroxene-type $NaScSi_2O_6$ (h) has also been included.

5). Furthermore, this confirms the results from bond valence calculations of considerably underbonded Na^+ in the $NaYSi_2O_6$ structure.

Discussion and Comparison with Related Structures

Concerning the more general aspects of the crystal chemistry of silicates, the present compound is by far not the only material containing unbranched *vierer* single chains. Examples include minerals such as batisite ($Na_2BaTi_2[Si_4O_{12}]O_2$),[37] haradaite ($Sr_2V_2[Si_4O_{12}]O_2$),[38] krauskopfite ($H_4Ba_2[Si_4O_{10}]\cdot 4H_2O$),[39] leucophanite ($Na_2Be_2Ca_2[Si_4O_{12}]F_2$),[40] and taikanite ($BaSr_2Mn_2[Si_4O_{12}]O_2$).[41] $Na_2Cu_3[Si_4O_{12}]$,[42] for instance, is a synthetically obtained member of this group. However, if the scope is extended to other tetrahedrally coordinated T cations, $\{\boldsymbol{uB},1^1_\infty\}$ $[^4T_4O_{12}]$ chains can be also found in vanadates ($K_2MnV_4O_{12}$)[43] or borophosphates ($Fe[B_2P_2O_7(OH)_5]$).[44] Figure 6 shows a comparison between the *vierer* single chains of different silicates. Most of the chains show a pronounced folding with stretching factors deviating significantly from 1.0, the value corresponding to a linear arrangement of the tetrahedra within the chain. With regard to the arrangement of the tetrahedra and the degree of folding, the chains present in $NaYSi_2O_6$ are similar to those in batisite. However, differences in linkage and stacking of the chains preclude a closer structural relationship between both compounds.

For the silicates with general composition $NaXSi_2O_6$ (X = trivalent cation), many different natural and synthetic representatives can be found. Almost all of these compounds belong to a family of chain structures named after the important rock-forming pyroxene mineral group, including X cations such as Sc, Ti, V, Cr, Al, In, Fe, and Ga.[45] Like scandium, yttrium belongs to subgroup IIIa of the periodic table of the elements, having similar electronic configurations in the outermost electronic shell. Furthermore, the oxide crystal chemistry of Sc^{3+} and Y^{3+} is comparable.[46,47] One could thus hypothesize that $NaYSi_2O_6$ should be somehow related to the pyroxene structure type. Concerning the general silicate anion type, this assumption is justified by the outcome of the present investigation: $NaScSi_2O_6$ and $NaYSi_2O_6$ both form tetrahedral single chains. However, when considering the chain architecture in more detail, we find that the two compounds differ considerably. Whereas the pyroxene family is characterized by slightly corrugated *zweier* single chains, the crystal structure of $NaYSi_2O_6$ contains *vierer* single chains showing a pronounced folding (see Figure 6). Furthermore, in contrast to the Y phase, the nontetrahedral cations in the sodium pyroxenes are octahedrally coordinated. For a plausible explanation of the structural differences, we have to look to the remaining significant chemical differences between the pyroxene-forming X cations and yttrium: the ionic radius and the electronegativity. In addition to the valence of an additional guest cation in a silicate, these two parameters are of special importance, and will greatly influence the topology that is adopted by a structure.[24] Through the use of databases for the ionic radii[48] and the electronegativities,[49] it becomes obvious that the size of Y^{3+} for a 6-fold coordination ($r^{[6]} = 0.900$ Å) is considerably larger than the corresponding values of all the elements listed above. On the other hand, the electronegativity of yttrium (EN = 1.22) is much lower than the electronegativities of the X cations. In this respect it is interesting to note that it is Sc (EN = 1.36) that has the lowest value of the elements forming $NaXSi_2O_6$ phases with pyroxene-type structures. Although the large size and the low electronegativity of yttrium seem to be an unfavorable combination for the formation of a sodium yttrium pyroxene at ambient pressure, it cannot be excluded that the application of high pressure

(34) Lasaga, A. C.; Gibbs, G. V. *Phys. Chem. Miner.* **1988**, *16*, 29−41.
(35) Frogner, P.; Broman, C.; Lindblom, S. *Chem. Geol.* **1998**, *151*, 161−168.
(36) Iishi, K.; Salje, E.; Werneke, C. *Phys. Chem. Miner.* **1979**, *4*, 173−188.
(37) Schmahl, W. W.; Tillmanns, E. *Neues Jahrb. Mineral., Monatsh.* **1987**, *1987*, 107−118.
(38) Takéuchi, Y.; Joswig, W. *Mineral. J.* **1967**, *5*, 98−123.
(39) Coda, A.; Dal Negro, A.; Rossi, G. *Atti Accad. Naz. Lincei, Cl. Sci. Fis., Mat. Nat., Rend.* **1967**, *series VIII 42*, 859−873.
(40) Canillo, E.; Giuseppetti, G.; Tazzoli, V. *Acta Crystallogr.* **1967**, *20*, 301−309.
(41) Armbruster, T.; Oberhänsli, R.; Kunz, M. *Am. Mineral.* **1993**, *78*, 1088−1095.
(42) Kawamura, K.; Kawahara, A. *Acta Crystallogr.* **1976**, *B32*, 2419−2422.
(43) Witzke, T.; Zhen, S.; Seff, K.; Doering, T.; Nasdala, L.; Kolitsch, U. *Am. Mineral.* **2001**, *86*, 1081−1086.
(44) Boy, I.; Hauf, C.; Kniep, R. *Z. Naturforsch.* **1998**, *53b*, 631−633.
(45) Ohashi, H. *J. Jpn. Assoc. Mineral., Petrol., Econ. Geol.* **1981**, *76*, 308−311.
(46) Gscheidner, K. A. *J. Less-Common Met.* **1971**, *25*, 405−422.
(47) Frondel, C. *Z. Kristallogr.* **1968**, *127*, 121−138.
(48) Shannon, R. D. *Acta Crystallogr.* **1976**, *A32*, 751−767.
(49) Pauling, L. *The Nature of the Chemical Bond*, 3rd ed.; Cornell University Press: Ithaca, NY, 1967.

may stabilize such a phase. High-pressure experiments are planned for the near future to settle this question.

Acknowledgment. The authors thank Bernhard Sartory for the electron microprobe analysis and for helpful discussions of the results.

Supporting Information Available: Crystallographic data for $NaYSi_2O_6$. This material is available free of charge via the Internet at http://pubs.acs.org.

IC051401O